Biomass Conversion and Biorefinery (2023) 13:3849–3862
https://doi.org/10.1007/s13399-021-01474-1

ORIGINAL ARTICLE

Pilot-scale biomass gasification system for hydrogen production from palm kernel shell (part A): steady-state simulation

Maham Hussain [1,2] · H. Zabiri [1,3] · Fahim Uddin [4] · Suzana Yusup [1,5] · Lemma Dendena Tufa [6]

Received: 14 December 2020 / Revised: 23 March 2021 / Accepted: 26 March 2021 / Published online: 2 April 2021
© The Author(s), under exclusive licence to Springer-Verlag GmbH Germany, part of Springer Nature 2021

Abstract

Hydrogen (H_2) production via biomass gasification has demonstrated to be a viable method to obtain environmental-friendly fuel. In this paper, steady-state modeling of palm kernel shell (PKS) steam gasification pilot-plant is developed and validated using experimental data. The process optimization study for the gasification of PKS utilizing the coal bottom ash as a catalyst is conducted in the continuous advanced fluidized bed technology pilot-scale gasification plant to determine the optimum conditions to produce maximum H_2 and syngas composition. The optimum conditions for maximum H_2 and syngas composition are a temperature of 625 °C, PKS particle size of 1–2 mm, and coal bottom ash to PKS percentage of 7.5 %. The optimum operating condition results are then validated in the pilot-scale gasification system. Steady-state simulation of the pilot scale biomass gasification plant is then developed using Aspen Plus® and validated using the experimental data.

Keywords Palm kernel shell · Coal bottom ash · Steady-state simulation · Aspen Plus® · Gasification · Steady-state simulation

1 Introduction

Nowadays, biomass is abundantly available worldwide, and the majority is derived from agriculture crops [1]. Coconut and oil palm trees are considered among the world's main agricultural crops according to LMC International Ltd. [1]. It is reported that global crude palm oil production from coconut and oil palm trees are approximately 3.35 million tonnes and 60.86 million tonnes, respectively [1]. As a result, over 70% of solid wastes were generated from post-processing of products such as trunks, fronds, leaves, fruits, and shells [2, 3]. Among them, coconut shells (CSs) and palm kernel shells (PKSs) have been considered as potential biomass fuels because of their syngas higher heating values (HHV) among all the agricultural solid wastes produced [2, 3]. Biomass gasification is one of the most efficient conversion technologies among thermochemical processes due to lower capital cost while retaining the potential for high-rate production of fuel gas [4]. Gasification performance is influenced by many factors, including the chemical and physical properties of biomass [5], gasifier design [6], and operational conditions, such as temperature [7], equivalence ratio [8], and gasifying agent [9]. Currently, various commercial gasifier designs, such as updraft, downdraft, and fluidized-bed gasifier, have been developed. Of the developed gasifiers, the downdraft gasifier is the most sustainable for combined heat and power generation because of the low tar and particulate composition in the produced syngas. Hydrogen plays an important role as fuel due to its high-energy content and low-emission concerns [10]. Hydrogen produced from biomass gasification can directly be used as a proton exchange membrane (PEM) fuel feedstock and to produce numerous chemicals such as methanol [10].

✉ H. Zabiri
haslindazabiri@utp.edu.my

1 Department of Chemical Engineering, Universiti Teknologi PETRONAS, 32610 Bandar Seri Iskandar, Perak, Malaysia

2 Department of Chemical Engineering, National Fertilizer Coorporation NFC (IET), Multan, Punjab, Pakistan

3 CO2 Research Center (CO2RES), Institute of Contaminant Management, Universiti Teknologi PETRONAS, 32610 Bandar Seri Iskandar, Perak, Malaysia

4 Department of Chemical Engineering, NED University of Engineering & Technology, Karachi, Pakistan

5 Department of Chemical Engineering, HICoE, Centre for Biofuel and Biochemical Research, Institute of Self-Sustainable Building, Universiti Teknologi PETRONAS, 32610 Bandar Seri Iskandar, Perak, Malaysia

6 School of Chemical and Bio-Engineering, Addis Ababa Institute of Technology, King George VI St Addis Ababa, 1000 Addis Ababa, Ethiopia

Gasification is the most promising technique for hydrogen production along with syngas [10].

Aspen Plus® has been widely employed to simulate chemical processes in a wide number of fields including but not limited to the petroleum industry, chemical processes, and biomass gasification. Modeling biomass gasification on the Aspen Plus® platform has gained momentum in recent years [11–14]. For biomass-gasification using Aspen Plus®, kinetic and thermodynamic equilibrium models are the most commonly used [15, 16]. The kinetic models consider the kinetics of the gasification reactions and the hydrodynamics of the gasification reactions [17]. The thermodynamic equilibrium model enables the composition of syngas to be predicted on the basis of the assumption that the reactants react for an infinite time in a totally mixed state [18]. This model is independent of the design of the gasifier and may therefore be more fitting for process studies on the effect of the various parameters of the process. There are two sub-categories of equilibrium models: stoichiometric models and non-stoichiometric models. Stoichiometric models are based on constants of equilibrium, so they need particular chemical reactions involved in the process. Non-stoichiometric models are based on the free energy minimization of Gibbs, and they provide the benefit of not taking chemical reactions into consideration. Many researchers have successfully used equilibrium models to model the gasification process in fluidized-bed gasifiers [4, 19, 20].

Doherty et al. [12] developed a model of wood chips biomass in Aspen Plus for a fast internally circulating fluidized bed (FICFB) gasifier. The results show that reactor temperature is the most important factor in syngas output, and the gasifier should be controlled between 850 and 950 °C. Furthermore, while the steam to biomass ratio has a major impact on lower heating value, it has a small impact on cold gas production. Begum et al.[21] developed an Aspen Plus model for an integrated fixed bed gasifier and predicted the steady-state performance of the model for different biomass feedstocks such as municipal solid wastes, wood wastes, green wastes, and coffee bean husks. It is observed that operating parameters have significant effect on the composition of syngas for each of the different feedstock. Sreejith et al. [22] on the other hand developed an equilibrium model based on Gibbs free energy minimization for steam gasification of wood using the Aspen Plus® process simulator to determine the optimum process conditions (pressure, temperature, and steam to biomass ratio). The simulation results of the Aspen Plus model are compared to those of another Gibbs free energy model built in MATLAB using the SA algorithm. In addition, Nikoo and Mahinpey [23] developed a model for the pinewood gasification in an atmospheric fluidized bed gasifier. The results showed that temperature enhances hydrogen production and increases carbon conversion efficiency. Carbon dioxide production and carbon conversion efficiency are directly proportional to the equivalence ratio. Increasing the ratio of steam to biomass increases the production of hydrogen and carbon monoxide and reduces the efficiency of carbon dioxide and carbon conversion. In their study, average particle size in the 0.25–0.75 mm range does not probably contribute significantly to the composition of product gases. Im-orb et al. [24] developed a model for biomass gasification combined with a Fischer-Tropsch (FT) process using Aspen Plus to perform a techno-economic analysis of the integrated process with rice straw feedstock for green fuel production. As the FT reactor volume increases at a constant recycle fraction, the CO conversion and diesel output rate from an FT synthesis unit increase, while the electricity generation decreases. By changing the FT off-gas recycle fraction and determining the FT reactor volume, the useful products from the BG-FT process, such as diesel and electricity, can be maximized. From the work of Ivana Cekovic et al. [25], a thermochemical equilibrium model is formulated for wood chips downdraft gasification. Steady-state Aspen Plus® simulator is utilized to evaluate the produced gas composition and low heating value. The equivalence ratio ranges from 0.32 to 0.38, and the air-fuel ratio varies from 1.49 to 1.81, when the performance of the gasifier is optimum, at 250 kW. Juan Manuel de Andres et al. [26] developed a model to simulate the sewage sludge gasification in an atmospheric fluidized bed gasifier using Aspen Plus. It is observed that operating at higher temperatures results in higher efficiency in H_2 and CO production. The use of air and steam as a gasifying agent increased the H_2 content of the emitted gases while lowering the temperature. Mahmut Acar et al. [27] considered the bubbling fluidized bed gasifier (BFBG) to specify an appropriate model for almond shell gasification. The chemical equilibrium model (CEM) and restricted chemical equilibrium method (RCEM) are developed using Aspen Plus®. The results showed that increasing temperature has been shown to increase cold gas efficiency (CGE) while having a negative impact on lower heating value (LHV). Above 850 °C, the gas heating value and CGE do not change significantly. Both the ratio of steam to biomass (S/B) and the content of biomass moisture have a useful effect on the production of H_2. However, these factors have a negative influence on the heating gas value. Im-orb et al. [28] developed an Aspen Plus model integrated with thermodynamic equilibrium for rice straw gasification in a bench-scale two-stage gasifier. It is observed that at low temperatures, the syngas yield of the two gasification processes increases significantly until it reaches a maximum value and is stable at temperatures above 700 °C. Tapas Kumar Patra et al. [29] developed a process model of the hydrogen-rich gas production through cleaning and catalytic conditioning of producer gas using Aspen Plus®. The results showed that the maximum composition of H_2 and CO conversion predicted by the model is 27.029 percent and 97.5479 percent, respectively, and the corresponding operating conditions are reactor, 350 °C

temperature, 8 S/CO, and 1000 h^{-1} GHSV. Beheshti et al. [30] developed a model to simulate air-steam gasification of biomass in a bubbling fluidized bed for hydrogen and syngas production. The results show that high temperatures are more favorable for the production of useful syngas (H_2 and CO) and for the production of hydrogen (HY). Mauro Villarini et al. [31] presented a study of biomass waste to energy conversion using gasification and internal combustion engine for power generation. The biomass waste analyzed is the most produced on Italian soil, chosen for its suitable properties in the gasification process. Recently, the configurations of various parameters on the processing of gases and the simulation of the process have also been studied in other research works [32–35].

In a biomass gasification process, the bio-hydrogen gasifier is one of the most important processing units. The gasifier performance is influenced by many factors, especially the operational conditions, such as temperature, equivalence ratio (e.g., steam-to-biomass or air-to-biomass, etc.), as well as the choice of gasifying agent and the chemical and physical properties of the biomass. Variations in the feedstock are another key factor that affect the gasifier performance. Very limited studies are reported on the biomass gasification control studies as per our knowledge, and recently few researchers have reported literature on machine learning-based modeling of biomass gasification [36–38].

A number of researchers have reported on the control studies related to biomass plants; however, no work has been reported with regard to the bio-hydrogen gasifier. All the works reported so far are based on different feedstocks such as pulverized coal and biomass (coconut shell, wood) for different processes like solar gasification, methanol synthesis, and boiler combustion system. In addition, for a new feedstock like PKS, most studies reported are based on experimental analysis only. For example, Ahmad Zubair Yahaya et al. [39] conducted the gasification of coconut shell (CS), and palm kernel shell (PKS) is in a batch type downdraft fixed-bed reactor to evaluate the effect of particle size and temperature on gas composition and gasification performance. There is also very limited literature on the use of coal bottom ash in steam biomass gasification. Only Shahbaz et al. [40] studied the catalytic-sorbent-based steam gasification of PKS in a pilot-scale integrated fluidized bed gasifier and fixed bed reactor using coal bottom ash as a novel catalyst for cleaner and hydrogen and syngas production. The results showed that it improved the tar cracking and enriched hydrogen composition as an effective catalyst. As it is vital to control the gasifier operating conditions adequately under varying plant disturbances to achieve the required product gas composition especially for new feedstock such as PKS, this study aims to develop steady-state simulation model for the gasification system reported in Shahbaz et al. [40] using PKS with coal bottom ash.

Hence, the scope of this paper is two-folds:

1. To determine the optimum conditions of hydrogen (H_2) and syngas production using pilot-scale gasification system

- Experiments have been carried out using the bench-scale gasifier system to get higher purity and yield of hydrogen from PKS via catalytic steam gasification with in-situ CO_2 capture [40].
- The effect of different process variables such as temperature, steam to biomass ratio, coal bottom ash to biomass percentage, and biomass particle size on hydrogen content in the product gas in the fluidized bed gasifier is studied. Temperatures are varied in the range of 500–750°C, where higher gasification temperature is unfavorable for CO_2 adsorption reaction (carbonation reaction based on CaO). High fluidization velocity, ranging from 3 to 5 times of minimum fluidization velocity is considered, to ensure high mass and heat transfer coefficients in the reactor. Steam to biomass and coal bottom ash to biomass percentage are in the range of 0.5–2.5 wt/wt and 5%, 7%, and 10% wt/wt, respectively. Two biomass particle sizes i.e. 0.5-1 mm and 1.0-2.0 mm are studied.

2. Development of steady-state simulation model and its validation with the experiments

- To develop an Aspen Plus® simulation model using actual process specifications, operating condition, and palm kernel shell biomass and coal bottom ash in the pilot-scale biomass gasification plant.
- The simulation model is validated with experimentation performed on the pilot-scale plant from Step (1).

2 Characterization of physical and chemical properties of the palm kernel shell

Palm kernel shell used as feedstock was supplied by Kilang Sawit Nasaruddin Sdn Bhd located in Perak, Malaysia. These materials were sun-dried for 4–5 days and then dried in an oven to ensure removal of free and bounded moisture. The biomass was ground using a Fritsch 19/25 analytical mill and sieved into particle sizes ranging from 1 to 2.0 mm. The samples were kept in an airtight container to prevent additional moisture content from entering.

2.1 Characterization of palm kernel shell

The characterization analysis of PKS includes proximate analysis, ultimate analysis, and calorific value analysis of the PKS.

2.1.1 Ultimate analysis

The components such as carbon, hydrogen, nitrogen, sulfur, and oxygen contents on dry weight % were determined using the LECO CHNS 932 elemental analyzer. Approximately 3 mg of sample was placed into a silver capsule and analyzed in the elemental analyzer. The furnace temperature of the elemental analyzer was maintained at 800 °C.

2.1.2 Proximate analysis

The contents such as fixed carbon, volatile matter, and ash content on a dry basis were calculated using the thermogravimetric analyzer EXSTAR TG/DTA 6300 (Seiko Instrument Inc.).

In the test, approximately 5 mg of sample was placed in the furnace and heated from room temperature to 110 °C, in the presence of nitrogen 99.9% with a flow rate of 100ml min^{-1} in the TGA. A temperature of 110 °C is kept constant for half an hour to ensure moisture content was removed. Afterward, the nitrogen gas at a flow rate of 100 ml min^{-1} was supplied constantly, and the temperature was allowed to ramp from 110 to 1000 °C. The nitrogen supply was continued for 10 min at a temperature of 1000 °C for the volatile matters to release. The volatile matters were determined according to ASTM E-872 standards. Then, oxygen gas (99.9%) at 30ml min^{-1} was supplied instead of nitrogen and maintained for 15 min at 1000°C to evaluate the ash content according to ASTM D-31775-01 standard. Then, fixed carbon was calculated by subtracting 100% of the weight percentages of moisture, volatile matters, and ash. The analysis was repeated three times to obtain consistent results. The fixed carbon content of the PKS was calculated using the equation as follows:

Fixed carbon (wt.%) = 100 − (moisture + ash + volatile matter)(1)

2.1.3 Calorific value

Calorific value, which is also known as higher heating value, for the PKS was determined in a C5000 oxygen calorimeter using the ASTM D5865-03 procedure. Approximately 5mg of the PKS sample was placed in a crucible, and 99.9% oxygen was provided into the calorimeter. The combustion took place inside the decomposition chamber by burning the sample using a cotton thread attached to the ignition wire inside the chamber. The analysis was repeated three times to obtain consistent results.

3 Experimental

3.1 Experimental setup

The experiments are carried out in a continuous advanced fluidized bed technology pilot-scale gasification pilot scale plant at the University Teknologi PETRONAS, the same plant reported in [40]. The palm kernel shell used as feedstock is supplied by Kilang Sawit Nasaruddin Sdn Bhd located in Perak, Malaysia, and coal bottom ash is obtained from TNB Janamanjung Sdn Bhd, Malaysia. These materials are sun-dried for 4–5 days and then dried in an oven to ensure removal of free and bounded moisture.

The biomass is ground using a Fritsch 19/25 analytical mill and sieved into particle sizes ranging from 0.5 to 2.0 mm, which are 0.5–0.71, 0.71–1.0, and 1.0–2.0 mm. The coal bottom ash is ground to the particle size of 0.5 mm. The samples are kept in an airtight container to prevent additional moisture content from entering. The characterization analysis of PKS includes proximate analysis, ultimate analysis, and calorific value analysis of the PKS which are not covered in this paper. The overall block diagram of the pilot-scale gasification plant is as shown in Fig. 1. The overall process is composed of feed handling, gasification, cooling, and separation sections.

The gasification system consists of a fluidized bed reactor, a steam generation system, and a polishing reactor. The biomass gasification process takes place in the fluidized bed reactor consisting of sand as the bed material and steam as a gasifying agent. Figure 2 shows the configuration of the fluidized bed reactor. The process flow diagram of the gasification plant is illustrated in Fig. 3. The premixed PKS and bottom ash are fed into the feed handling system at the hopper. From there, it is fed into the gasification system via a screw feeder at a specified feed rate.

There are three main sections in the fluidized bed reactor which are the plenum, main bed, and the freeboard. The region overhead the distributor plate is the plenum, where bed material is allowed to fluidize, and the expanded zone above the main bed is the freeboard. There are three internal temperature indicators (TI) to monitor the internal temperatures of the reactor in the fluidized bed reactor. The total pressure drop across the reactor plenum and freeboard sections are monitored with two differential indicators (PDI). Four ceramic heaters are installed to heat the reactor. Other utilities in place include steam, a three phase 240 volts electricity supply, and a compressed N_2 supply. The specification of the fluidized bed reactor is summarized in Table 1.

The steam is produced by an electric boiler and further heated in a superheater until it reaches a temperature of 250–300 °C, until it is then injected into the fluidized bed reactor. From the fluidized bed gasifier, the gaseous product stream entered the gas cleaning system. It is composed of a cyclone where solid particulates like fine ash and dust particles are separated as flue from the gaseous product of the fluidized bed reactor. The cyclone is between the fluidized bed gasifier and polishing reactor. Heating tape is installed to avoid tar condensation on the cyclone pipelines. The gaseous product is passed through a scrubber after the polishing reactor to cool down the gaseous product to 40°C before entering the

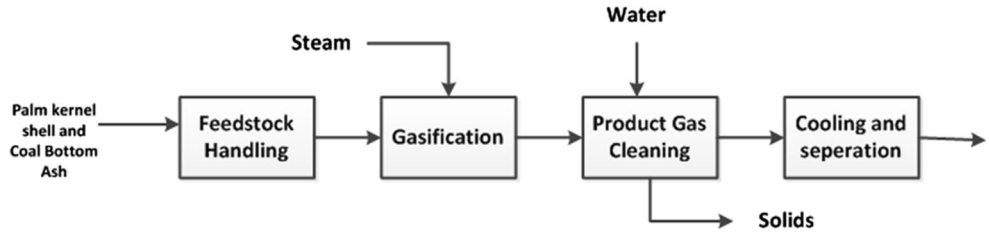

Fig. 1 Block diagram of pilot scale gasification system

analyzing system. A scrubber is used to remove fine particles of up to 0.5 μm and tar content from the gaseous product [41]. Afterwards, any remaining moisture is removed from the gaseous product in the separator section. Finally, a sample of the clean and moisture-free product gas is sent to the gas analyzing system.

The operating conditions of the fluidized bed reactor are as presented in Table 2.

3.2 Aspen Plus® model

In this study, Aspen Plus® model of the biomass gasification pilot-scale plant is developed. The development of the Aspen Plus model involved the following sequential steps: (1) stream class specification, (2) property method selection, (3) system component specification (from databank) and identifying conventional and non-conventional components, (4) defining the process flowsheet (using unit operation blocks and connecting material and energy streams), (5) specifying feed streams (flow rate, composition, and thermodynamic condition), and (6) specifying unit operation blocks (thermodynamic condition, chemical reactions, etc.). To simulate the reactor unit operation in Aspen Plus, a number of reactions are provided within the Aspen Plus input file. The assumptions considered in the simulation include the following: (a) the model is at steady state, kinetic free, and isothermal; (b) chemical reactions take place at an equilibrium state in the gasifier, and there is no pressure loss; (c) all elements (except sulfur content) take part in the chemical reaction; (d) all gases are ideal gases, including hydrogen (H_2), carbon monoxide (CO), carbon dioxide (CO_2), steam (H_2O), nitrogen (N_2), and methane (CH_4); and (e) char contains only carbon and ash in solid phase.

PENG-ROBINSON equation of state is used to estimate all physical properties of the conventional components in the Aspen Plus steady-state simulation. The PENG-ROBINSON equation (shown in (1)) is a version of the general cubic equation of state. At high temperature, this package improves the correlation of pure component vapor pressure which makes it suitable for the gasification process [38]:

$$p = \frac{RT}{(c + V_m) - b} - \frac{a}{(V_m + c)(V_m + c + b)(V_m + c - b)} \quad (1)$$

where a, b, and c are component-specific parameters. The values of these parameters are stored in Aspen Plus®. Table 3 tabulates the reactions (1)–(6) involved in the process.

The gasification process involved drying, decomposition, gasification, and combustion stages. Figure 4 shows the Aspen Plus simulation flowsheet of the biomass gasification plant. Biomass is defined as a non-conventional component in Aspen Plus and described by using the ultimate and proximate analysis. The model is based on the Gibbs free energy minimization and based on the assumption that sufficient residence time is provided to allow chemical reaction to attain equilibrium.

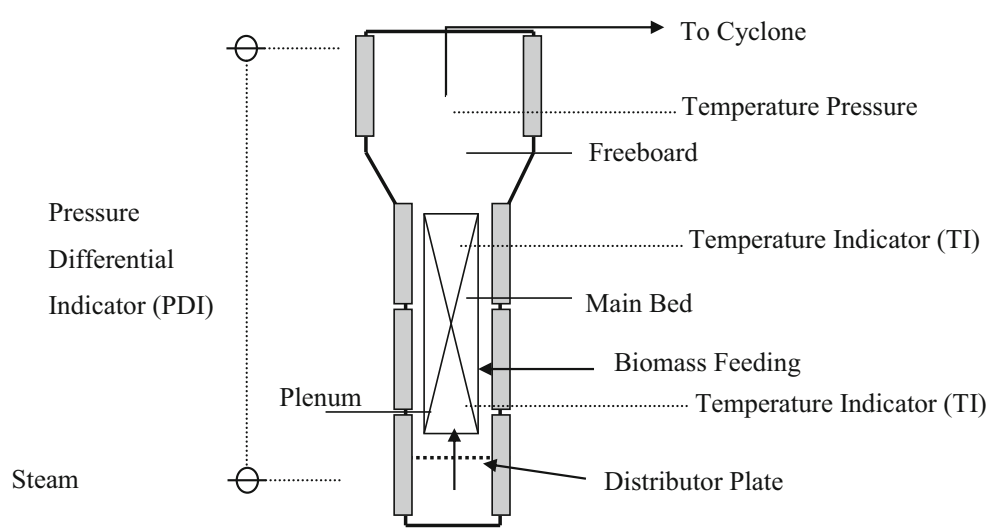

Fig. 2 Fluidized bed reactor configuration

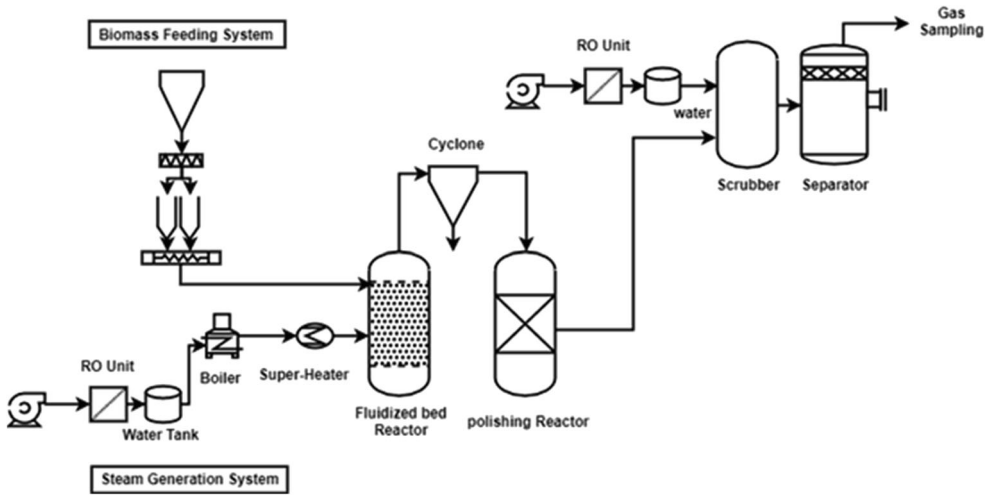

Fig. 3 Process flow diagram of pilot scale plant

The flowsheet in Fig. 4 represents a typical setup used in biomass experimental studies [40]. The unit operations block data are as follows:

- R-Gibbs: This model block is based on single-phase chemical equilibrium works on minimization of Gibbs free energy; this model has significance under known temperature and pressure with unknown stoichiometry.
- Split: Feed splitter divide the feed based on splits specified by outlet streams.
- Mixer: Mixes two or more streams. It can also combine material, heat, and work streams.
- Flash: It is generally known as a two-outlet flash. This model works on the principle of rigorous vapor-liquid or vapor-liquid-liquid equilibrium.
- Superheater: It increases the temperature of water to make it superheated steam.
- Cyclone: It separates solids from the product gas.

The overall gasification stages comprised of feed decomposition, devolatilization, and gas solid separation in the simulation model. The palm kernel shell (PKS) biomass as a feedstock (on a wt% dry basis) is fed at 1.35 kg/hr and (defined as a heterogeneous solid in Aspen Plus®). The physical properties of solids and non-conventional components are calculated using the Peng-Robinson-Boston-Mathias (PR-BM) model. This property package defined both the pure and mixed components properties. The HCOALGEN and DCOALIGHT property models are used to calculate enthalpy and density of the biomass, char, and ash-like components.

The steam is produced and provided by an electric boiler (E-401) and further heated in a superheater until it reaches a temperature of 300 °C, after which it is then injected into the reactor. In the model, an R-GIBBS operation block is used to convert biomass to syngas. The Aspen Plus R-GIBBS Reactor is used to perform the decomposition and gasification of PKS with the assumption that these reactions follow the Gibbs free energy minimization calculations. This step employed the decomposition of PKS into their constituent components, including carbon, hydrogen, oxygen, nitrogen, and sulfur, at a specified temperature and pressure. The combustible substances from R-GIBBS include H_2, CO, CO_2, and CH_4. Additionally, coal bottom ash is added to the reactor section and steam as a gasifying medium provided by an electric

Table 1 Biomass fluidized bed system specification

Parameter	Value
Internal diameter (ID) (m)	0.15
Total height (m)	2.50
Freeboard height (m)	0.40
Freeboard internal diameter (m)	0.20
Plenum height (m)	0.30
Distributor plate hole diameter (m)	0.0015
Feeding point location from the distributor (m)	0.20
Operating temperature (°C)	500–900
Preheat steam temperature (°C)	250–300
Operating pressure (bar)	1–6

Table 2 Fluidized bed reactor operating conditions

Parameter	Value
Biomass feed rate (g/h)	1000–1800
Steam flow rate (g/h)	2000–3500
Temperature (°C)	500–750
Pressure (bar)	1
Catalyst (wt/wt)	0.075
Steam to biomass ratio (wt/wt)	0.5–2.5
Bed material particle size (mm)	0.250
Biomass particle size (mm)	1.0–2.0

Table 3 Chemical reactions involved in PKS gasification [42–44]

No	Name	Reaction	ΔH (KJ/mol)
1	Char gasification	$C_{4.15}H_{6.13}O_{2.73}+1.44H_2O \leftrightarrow 4.25H_2+4.15CO$	131.50
2	Methanation	$C_{4.15}H_{6.13}O_{2.73}+8.2H_2 \leftrightarrow 4.15CH_4+2.71H_2O$	−74.80
3	Boudouard	$C_{4.15}H_{6.13}O_{2.73}+CO_2 \leftrightarrow 2.25H_2+4.15CO+0.56H_2O$	172.00
4	Methane reforming	$CH_4+H_2O \leftrightarrow CO+3H_2$	206.00
5	Water gas shift	$CO+H_2O \leftrightarrow CO_2+H_2$	−41.00
6	Carbonation	$CO_2+CaO \leftrightarrow CaCO_3$	−170.50

boiler (E-401) and further heated in a superheater until it reached a temperature of 300 °C. It is then supplied to the bottom of the gasifier, where it reacted with the biomass. All reactions in the gasification process are assumed to reach chemical equilibrium before the syngas leaves the reactor. Thermodynamically, the total Gibbs free energy of a closed system at a constant temperature and pressure must decrease during an irreversible process. Additionally, the gas product is supplied further to Gasifier-2 for carbon dioxide capture. On the other hand, the gaseous product is passed through a scrubber (E-402) after the polishing reactor (R-406) to cool down the gaseous product to 40 °C before entering the analyzing system. Afterward, any remaining moisture is removed from the gaseous product in the separator section(S-401).

A gas-liquid absorber is used for the separation of liquid and gas (syn. gas) products at atmospheric conditions. An analyzer has been used to determine the composition of the subsequent gases, i.e., H_2, CO, CO_2, and CH_4.

3.2.1 Model validation

In the experimental analysis described in the previous section, the process optimization study for the gasification of PKS utilizing the coal bottom ash as a catalyst is conducted in the continuous advanced fluidized bed technology pilot-scale gasification plant to determine the optimum conditions to produce maximum H_2 and syngas composition. The effect of different process variables such as temperature, steam to biomass ratio, coal bottom ash to biomass percentage, and biomass particle size on H_2 content in the product gas in the fluidized bed gasifier is studied. Temperatures are varied in the range of 500–750°C, where higher gasification temperature is unfavorable for CO_2 adsorption reaction (carbonation reaction based on CaO). High fluidization velocity, ranging from 3 to 5 times of minimum fluidization velocity, is considered, to ensure high mass and heat transfer coefficients in the reactor. Steam to biomass and coal bottom ash to biomass percentage are in the range of 0.5–2.5 wt/wt and 5%, 7%, and 10% wt/wt, respectively. Two biomass particle sizes, i.e., 0.5–1 mm and 1.0–2.0 mm, are evaluated.

After the optimum conditions have been determined experimentally for maximum H_2 and syngas composition, steady-state simulation of the pilot scale biomass gasification plant is then developed using Aspen Plus® based on the obtained optimum conditions. Once the steady-state simulation has converged based on the experimentally obtained optimum conditions, the Aspen Plus® model is then used to study the effect of the gasifier temperature and steam/biomass on syngas compositions and validated with the experimental data. To evaluate the reliability of the simulation results, the prediction accuracy is then evaluated using the sum-squared deviation errors defined in (2) to (4):

$$RSS = \sum_{i=1}^{N} \left(\frac{y_{ie} - y_{ip}}{y_{ie}} \right)^2 \quad (2)$$

e experimental
P predicted

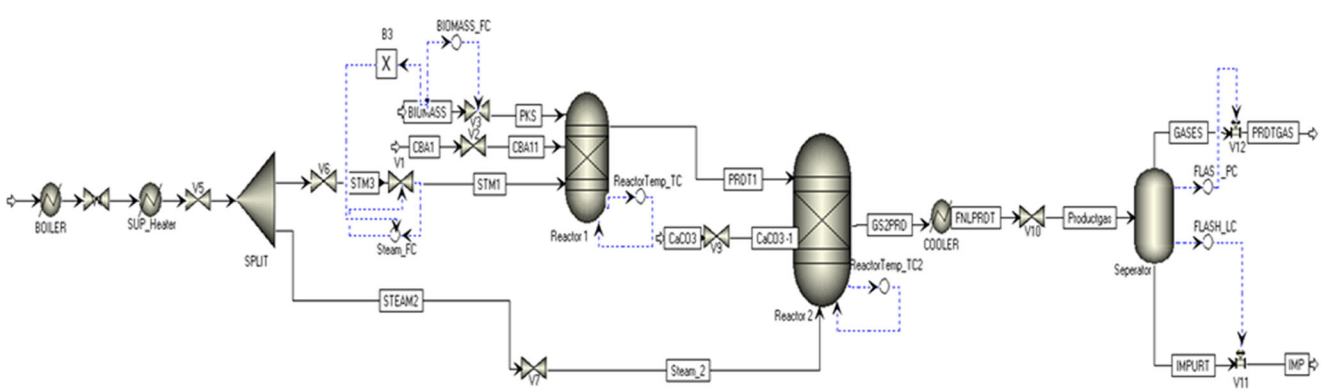

Fig. 4 Aspen Plus® simulation schematic flowsheet for PKS gasification

$$MRSS = \frac{RSS}{N} \quad (3)$$

$$\text{Mean Error} = \sqrt{MRSS} \quad (4)$$

3.2.2 Gaseous product composition

The gaseous product composition is an important parameter that will define the performance of the gasification process by analyzing the gas composition of the H_2, CO, CO_2, and CH_4 gas produced from the gasification process. Each gas component is reported by vol.% as represented in (5):

$$\text{Vol.\%} = \frac{\text{Volume of gas}(m^3)}{\text{Total volume of product gas } (m^3)} \quad (5)$$

4 Results and discussions

4.1 Characterization of biomass feedstock (PKS)

The properties of PKS ultimate analysis, proximate analysis, and calorific value are presented in this section.

4.1.1 Ultimate analysis

The ultimate analysis for PKS is presented in Table 4. The results show high carbon content, i.e., 45.66±0.44 wt% in the PKS. The high carbon content is present in products like methane, solid char, and high hydrocarbons (tar and light gases), when they undergo a devolatilization process. The char and methane produced reacts with the steam in the char gasification and methane reforming reactions to produce H_2-rich gas. Moreover, the higher amount of carbon in comparison to H_2 and oxygen results in higher calorific value of the fuel, as there are higher energy content in carbon-carbon bonds compared to carbon-oxygen and carbon-hydrogen bonds [45]. The low sulfur and nitrogen contents produced a lesser amount of NO_x and SO_x compositions in the product. The low amount of nitrogen and sulfur content in palm kernel shell are 0.66±0.07 and 0.46±0.05 wt%, respectively.

Table 4 Ultimate analysis for palm kernel shell (PKS)

Ultimate analysis (wt. %)	
Carbon (C)	45.66±0.44
Hydrogen (H)	6.82±0.38
Nitrogen (N)	0.66±0.07
Sulfur (S)	0.46±0.05
Oxygen (O) (by difference)	46.41±0.94

Table 5 Proximate analysis of PKS

Proximate analysis (wt. %)	
Moisture content	4.61±0.32
Volatile matter	72.40±0.50
Ash content	1.42±0.41
Fixed carbon (by difference)	21.60±0.35

4.1.2 Proximate analysis

The proximate analysis of PKS is presented in Table 5. The results show a moisture content of 4.6±0.32. The moisture content for the biomass feedstock used in biomass gasification should be less than 30% in order to achieve acceptable ignition and acceptable calorific value from the product gas [46]. The feedstock with a higher amount of moisture content can decrease the temperature achieved in the oxidation zone and will result in an incomplete tar cracking in the pyrolysis zone, leading to high tar content in the product gas [46]. Furthermore, volatile matter and ash content present are 72.4 ±0.50 and 1.4±0.41 wt%, respectively. The high volatile matter and low ash content allow for the gasification process to be operated at a lower temperature range of (600–750°C) [47]. The lower amount of ash content provides a benefit for the gasification feedstock because it helps to avoid agglomeration and slugging problems in the pipelines that can cause blockage along the pipelines [46]. Also, there is no need to install an ash removing system for the gasification system and save capital cost [47].

4.1.3 Calorific value

The heating value of PKS is presented in Table 6. The result shows that the calorific value of PKS is 17.05 MJ/Kg. The calorific value is affected by the moisture content present in the feedstock. The moisture content of the feedstock is low; therefore, a high calorific value is predictable from the feedstock. The presence of low moisture content in the feedstock will require less energy or heat to remove the excess moisture in the combustion process. Consequently, it increases the overall heating value of the feedstock.

Table 6 Higher heating value of PKS

Parameter	Value (MJ/Kg)
High heating value (HHV)	17.00

Table 7 Optimum condition for H_2 composition validation

Input parameters	Experimental run			
	First run (vol %)	Confirmation run (vol %)		
		1	2	3
H_2 composition	81.20	81.76	80.61	78.20

4.1.4 Reproducibility of experimental results

Based on the process optimization study performed in the continuous advanced fluidized bed technology pilot-scale gasification plant as described in Section 3.3.2 and earlier, the optimum conditions for maximum H_2 and syngas composition are a temperature of 625 °C, PKS particle size of 1–2 mm, and coal bottom ash to PKS percentage of 7.5 %. The optimum operating condition results are then validated in the pilot-scale gasification system via three times experimental repetitions. The results of the reproducibility analyses are shown in Table 7. The three points are taken to highlight the trend within minimum to maximum ranges of parameters. Kindly note that in between many data sets are recorded during experimentation.

4.2 Steady-state simulation results

4.2.1 Effect of gasifier temperature on synthesis gas composition

Among all the variables, temperature is found to be the most significant factor that influenced the biomass gasification process. The effect of temperatures from 500 to 750°C on product gas composition at a steam to biomass ratio of 1.25 and coal bottom ash to PKS of 7.5% is as shown in Figs. 5, 6, 7, and 8. In Figs. 5, 6, 7, and 8, performance behavior of the Aspen Plus simulation results and actual experimental data are shown for H_2, CO, CH_4, and CO_2 compositions for temperatures in the range of 500–750°C.

It is observed that H_2 concentration increases with the increase in temperature from 500 to 625°C however decreased at a higher temperature of 750°C. Figure 5 shows reasonable agreement between the simulation results and the experimental data for H_2 production in temperatures higher than 600 °C. As the biomass produces more tar and unburned hydrocarbon at lower temperatures, less H_2 will consequently be produced. The increase in H_2 content is due to the water gas shift reaction $CO+H_2O \leftrightarrow CO_2+H_2$ and steam methane reforming reaction $CH_4+H_2O \rightarrow CO+3H_2$ at a temperature range of 500−625 °C. The water gas shift reaction produces CO_2, and the amount reduces with increasing temperature. This is due to the Boudouard reaction, which becomes dominant and

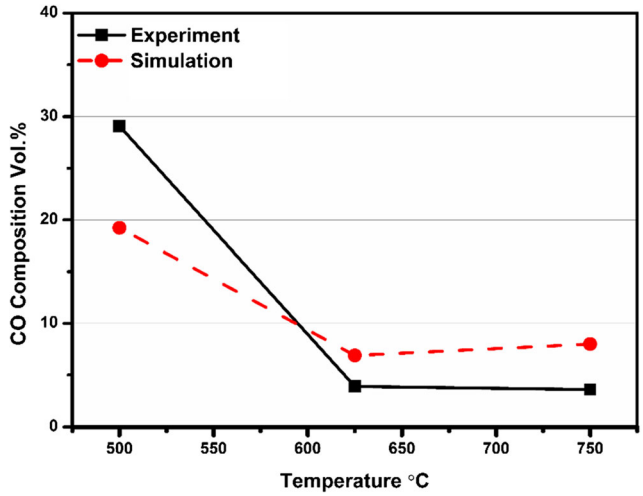

Fig. 6 Effect of temperature on CO (steam/biomass ratio=1.25, catalyst to biomass %=7.5)

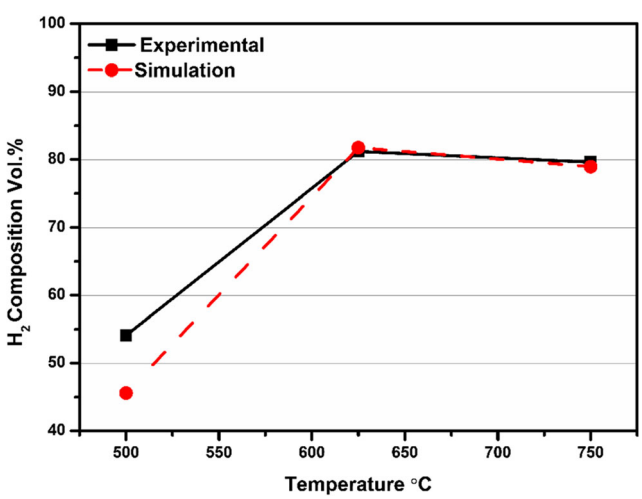

Fig. 5 Effect of temperature on H_2 (steam/biomass ratio=1.25, catalyst to biomass % = 7.5)

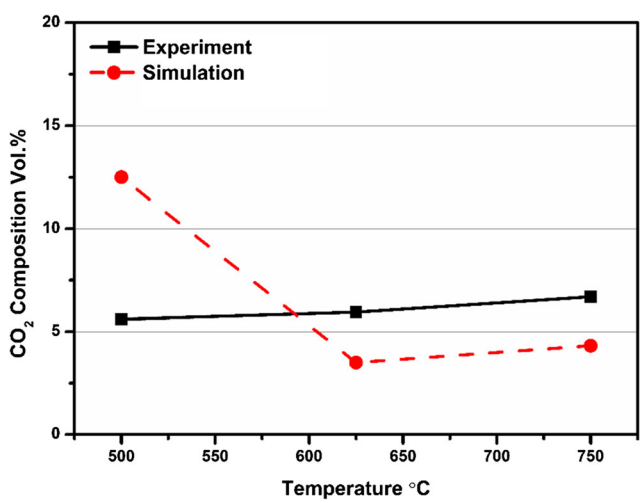

Fig. 7 Effect of temperature on CO_2 (steam/biomass ratio=1.25, catalyst to biomass %=7.5)

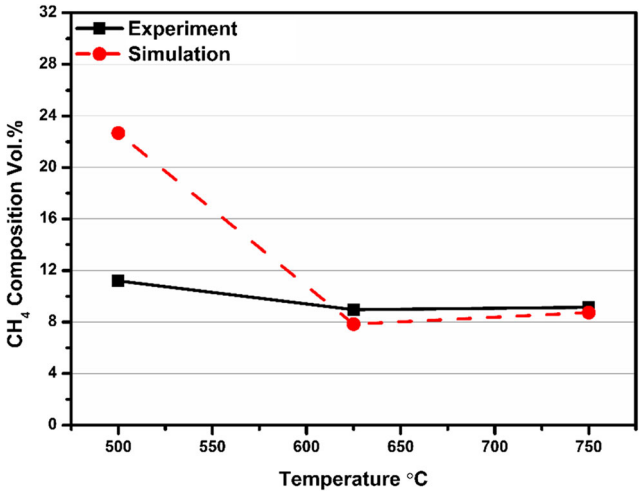

Fig. 8 Effect of temperature on CH_4 (steam/biomass ratio=1.25, catalyst to biomass %=7.5)

consumes CO_2. In the current study, it is clear that as the temperature increases, water gas shift reaction becomes dominant in the range of 600–625°C. In Fig. 6, the composition of CO decreased from 20.1 to 8.0 vol% when the temperature is increased from 500 to 750°C.

Similar results have been reported for reactor temperature effect on H_2 composition using CaO [48], which also shows that H_2 and CO content decreased at higher temperatures due to the presence of CaO [2]. The utilization of both an adsorbent and catalyst produced a higher H_2 composition, as demonstrated by biomass catalytic steam gasification and steam gasification with in situ CO_2 adsorbents [49]. The CaO as an adsorbent has a significant impact on syngas composition in the gasification process, because it captures the CO_2 from the product gas. In this study, CaO used as an adsorbent for CO_2 adsorption promotes the water gas shift reaction and steam methane reforming reaction in the gasification [50]. The use of CaO increased the H_2 content due to the catalytic effects of methane reforming and tar cracking reactions, which in turn also facilitates the CO_2 capture [51, 52].

In Fig. 7, it is observed that CO_2 content decreased with an increase in temperature from 500 to 625 °C, and then a reversible effect is observed after 700 °C. The decrease in CO_2 content is due to carbonation reaction supported by the presence of CaO as shown in the following equation [53]:

$$CaO + CO \rightarrow CaCO_3 \quad \Delta H = -170.5\ KJ/mol$$

The CaO adsorbs the CO via water gas shift reaction, in which it reacts with CO_2 and results in $CaCO_3$ formation. With increasing temperature, the CO_2 increases due to the reverse exothermic carbonation reaction, as followed by Le Chatelier's Principle for the following equation:

$$CaCO_3 \rightarrow CaO + CO_2 \quad \Delta H = -170.5\ KJ/mol$$

Rupesh et al. [53] also reported the deactivation of CaO at a high temperature of 727 °C in the sorption supported biomass gasification. A similar effect of carbonation reaction at the high temperature of 727 °C was observed by Xu et al. [54].

As shown in Fig. 8, the amount of CH_4 decreased from 23.4 to 10.1 vol.% as the temperature increased from 500 to 750 °C. It is due to the increase in methane reforming reaction with an increase in temperature, due to presence of steam [43, 55].

Table 8 summarized the comparison between the simulation and experimental data for the variation in temperatures.

It can be noted that the composition of H_2 at lower temperature, i.e., 500°C is relatively lower, and the deviation observed between the experimental and simulation output is greater. On the other hand, at higher gasification temperatures (625°C, 700°C), satisfactory agreement between the simulation and experiments is seen. The increase in H_2 composition with the increase in temperature is because of the water gas and the Boudouard reactions which are favored at higher temperatures due to which there is a lesser amount of H_2 content at temperature 500°C. The deviation between the experimental and simulation results is higher at lower temperature due to the assumption in the simulation that the effect of tar is negligible and Char contains only carbon and ash in the solid phase. The same assumption is also reported for biomass gasification simulation using Aspen Plus® software in the literature [53, 56]. At lower temperature, the presence of unconverted carbon is higher in the experimental set-up resulting in the lower

Table 8 Comparison of synthesis gas composition from simulation and pilot-plant experimentation data with temperature variation

Components	Temperature						
	500 °C		625 °C		750 °C		
	Sim.	Exp.	Sim.	Exp.	Sim.	Exp.	Overall mean error
H_2	54.10	45.60	81.20	81.76	79.61	78.95	0.1078
CO	19.23	29.10	6.90	3.90	8.00	3.59	0.8594
CO_2	12.50	5.60	3.50	5.94	4.32	6.69	0.7772
CH_4	22.67	11.20	7.84	8.96	8.73	9.15	0.5962

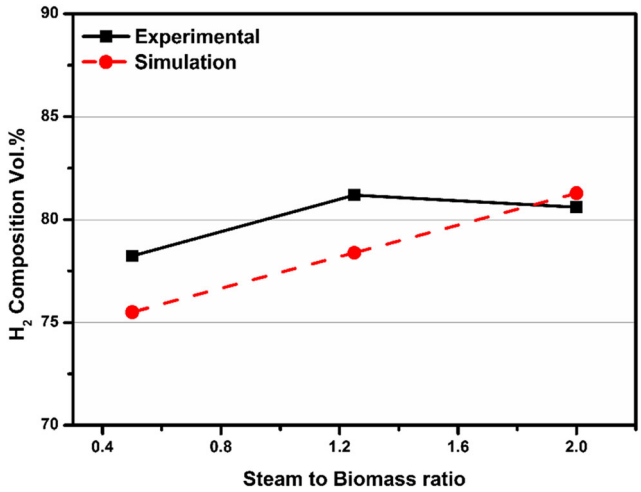

Fig. 9 Effect of steam/biomass on H_2 (temperature=625 °C, catalyst to biomass %=7.5)

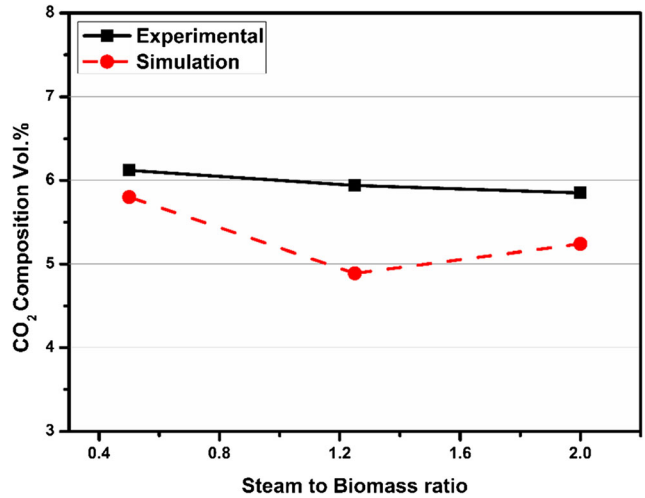

Fig. 11 Effect of steam/biomass on CO_2 (temperature=625 °C, catalyst to biomass %=7.5)

amount of H_2 and syngas, as is evident by the chemical reactions. Within this lower temperature region, the simulation model overestimated the H_2 and syngas amounts due to the assumption that Char contains only carbon and ash in the solid phase as Aspen Plus does not facilitate solids [57]. In contrast, the simulation results agree with the experimental results at higher temperatures.

4.2.2 Effect of steam/biomass on syngas composition

Steam as a gasifying agent has an important effect on syngas composition. In this study, steam/biomass ratio is varied from 0.5 to 2.5, and its effect on syngas composition is observed. Figures 9, 10, 11, and 12 compare the simulation predictions with experimental results of gas compositions versus steam to biomass ratio at three points in the range of 0.5–2.5. The effect of steam to biomass ratios on H_2 composition is shown in Fig. 9.

It is shown in Fig. 9 that H_2 composition increased as the steam to biomass ratio increases from 1 to 1.5. It is due to the higher activity of water gas shift reaction, char gasification, and steam reforming of methane. Many researchers also reported the activity of these reactions in the direction of H_2 content [2, 53]. Due to steam, the H_2 content increased and shifted the water gas shift reaction equilibrium in the forward direction [58]. In comparison to air gasification, steam as a gasifying agent produces more H_2 content in the syngas [59].

Figure 10 shows the corresponding effect on CO composition. It is found that CO composition decreases with an increase in steam to biomass ratio due to the higher activity of steam methane reforming reaction in the presence of steam. Moreover, a slight decrease in CO_2 content with increase in steam to biomass ratio is observed in Fig. 11. It may be probably be due to the decrease in CO and CH_4 contents (as shown

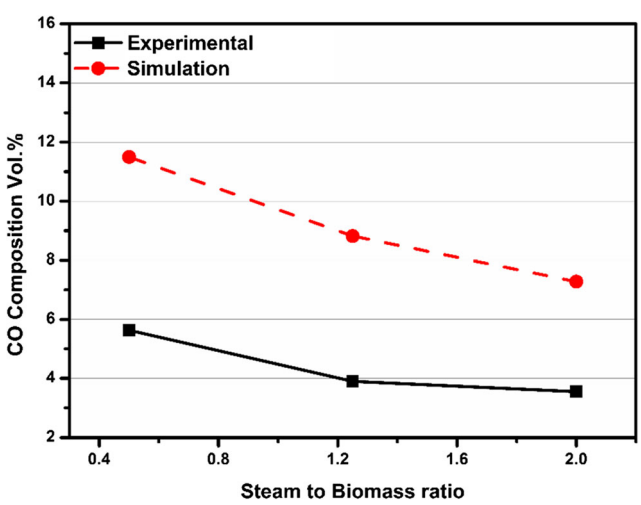

Fig. 10 Effect of steam/biomass on CO (temperature=625 °C, catalyst to biomass %=7.5)

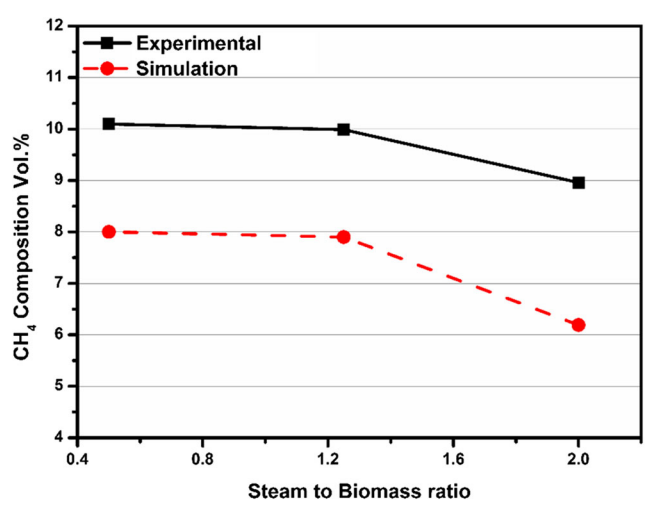

Fig. 12 Effect of steam/biomass on CH_4 (temperature=625 °C, catalyst to biomass %=7.5)

in Figs. 10 and 12, respectively) which accelerated the water gas shift and steam methane reforming reaction activity.

Khan et al. [55] reported similar justifications for an increase in CO_2 composition in the presence of CaO. Acharya et al. [48] observed the similar trend in CO_2 content for the steam gasification of sawdust. Rupesh et al. [53] also reported the same phenomenon in their air-steam sorption enabled gasification model.

The effect of steam to biomass ratio is important for syngas production, as excess amount of steam can decrease the gasification temperature [60]. The higher syngas composition is due to the presence of Al_2O_3, Fe_2O_3, and MgO in the coal bottom ash for catalytic steam gasification. The Fe_2O_3 and Al_2O_3 contents enhanced the char gasification [61]. Xiong et al. [62] investigate the coal bottom ash as the bed material in a fluidized bed reactor. It is reported that its use reduced the tar yield significantly. This effect is due to the metal compounds existing in the coal bottom ash (Fe_2O_3, Fe_3O_4, CaO, $CaSO_4$, etc.). Therefore, the use of coal bottom ash is important in the enhancement of syngas composition and decrease in tar content and higher gasification efficiency [63]. The H_2 content increased, while CO, CO_2, and CH_4 contents decreased. The increase in H_2 contents is due to the water-gas shift reaction (7) and steam reforming reaction (9). The use of coal bottom ash for decrease in tar reduction is also observed in the pyrolysis of coal [61]. The catalyst improved the solid carbon conversion into the gaseous product and also enhanced the tar cracking which results in an enhanced H_2 content in the syngas.

In the case of steam to biomass ratio, the trends observed in the simulation results for H_2, CO, CO_2, and CH_4 validate well with the trends shown by the experimental results as shown in Figs. 9, 10, 11, and 12. With the increase in the steam to biomass ratio, there is a sufficient amount of steam to maintain the temperature inside the reactor to breakdown the char and for the reaction to proceed adequately. The subsequent decrease in the trend is due to the excess amount of water content leading to the reduction in the temperature of the reactor [60]. The comparative error analysis between the simulation and experimental results tabulated in Table 9 indicates that higher accuracy is observed in the H_2 composition. In contrast, relatively higher errors are observed especially in terms of CO composition at lower steam to biomass ratio (less than 2.0). Similar to the effect of the lower temperature region explained in the previous section, the overestimation of the CO amount is probably due to the assumption that Char contains only carbon and ash in the solid phase as Aspen Plus does not facilitate solids [57].

5 Conclusions

In this current work, the optimum conditions for maximum H_2 and syngas composition of a steam gasification pilot-plant using palm kernel shell (PKS) with CaO and coal bottom ash have been obtained experimentally. The optimum conditions for maximum H_2 and syngas composition obtained are 625 °C, PKS particle size of 1–2 mm, and coal bottom ash to PKS percentage of 7.5 %. A steady-state model of the palm kernel shell (PKS) gasification pilot-plant is then developed in Aspen Plus® based on the Gibbs free energy minimization method using the optimum conditions. Validation of the developed simulation model has been carried out by varying the temperatures from 500 to 750°C on product gas composition at fixed steam to biomass ratio of 1.25 and coal bottom ash to PKS of 7.5%, as well as by varying the steam/biomass ratio from 0.5 to 2.5 at fixed temperature of 625 °C and coal bottom ash to PKS of 7.5%. Results show that within the lower temperature region (500°C), the simulation model generally tends to overestimate the H_2 and syngas amounts due to the assumption that Char contains only carbon and ash in the solid phase as Aspen Plus does not facilitate solids. In contrast, the simulation results agree with the experimental data at higher temperatures. With respect to the effect of varying steam to biomass ratio, higher prediction accuracy of the simulation results is observed in the H_2 composition. However, relatively higher prediction errors are observed in CO, CO_2, and CH_4 especially at lower steam to biomass ratio, probably due to the same assumption on the Char contents made previously. As reasonable agreement can generally be deducted between the simulation and experimental results, the steady-state model may be used for future dynamic and control studies of the pilot-plant

Table 9 Comparison of synthesis gas composition from simulation and pilot-plant experimentation data with steam/biomass variations

Components	Steam/biomass						
	0.5		1.25		2.5		
	Sim.	Exp.	Sim.	Exp.	Sim.	Exp.	Overall mean error
H_2	75.50	78.23	78.39	81.20	81.29	80.61	0.03
CO	11.50	5.63	8.82	3.90	7.28	3.55	1.123
CO_2	5.80	6.12	4.89	5.94	5.24	5.85	0.12
CH_4	8.00	10.10	7.90	9.99	6.19	8.96	0.25

gasification system. The steady-state simulation model may then be exported to ASPEN-DYNAMICS simulation which is then used for studying the dynamic behavior of the gasification system. Advanced model-based control studies may be explored using the Aspen-Dynamics simulation model to evaluate the efficacy against traditional control strategies such as Proportional-Integral-Derivative (PID) controllers.

Nomenclature *HHV,* higher heating value, MJ/kg; *LHV,* lower heating value, MJ/kg; *T,* temperature, °C; CO_2, carbon dioxide; *CO,* carbon mono oxide; CH_4, methane; H_2, hydrogen; *SBR,* steam to biomass ratio; *PKS,* palm kernel shell; *CGE,* cold gas efficiency

Acknowledgements The authors gratefully acknowledge the financial grant by the Universiti Teknologi PETRONAS.

References

1. Wahab AG (2015) Malaysia Oilseeds and Products Annual. GAIN Report Number: MY4006. USDA Foreign Agricultural Service. Kuala Lumpur, Malaysia, 2014
2. Khan Z, Yusup S, Ahmad MM, Rashidi NA (2014) Integrated catalytic adsorption (ICA) steam gasification system for enhanced hydrogen production using palm kernel shell. Int J Hydrog Energy 39(7):3286–3293
3. Kong M, Fei J, Wang S, Lu W, Zheng X (2011) Influence of supports on catalytic behavior of nickel catalysts in carbon dioxide reforming of toluene as a model compound of tar from biomass gasification. Bioresour Technol 102(2):2004–2008
4. Marcantonio V, De Falco M, Capocelli M, Bocci E, Colantoni A, Villarini M (2019) Process analysis of hydrogen production from biomass gasification in fluidized bed reactor with different separation systems. Int J Hydrog Energy 44(21):10350–10360
5. Singh VCJ, Sekhar SJ (2016) Performance studies on a downdraft biomass gasifier with blends of coconut shell and rubber seed shell as feedstock. Appl Therm Eng 97:22–27
6. Kumar A, Jones D, Hanna M (2009) Thermochemical biomass gasification: a review of the current status of the technology. Energies 2(3):556–581
7. Taba LE, Irfan MF, Daud WAMW, Chakrabarti MH (2012) The effect of temperature on various parameters in coal, biomass and CO-gasification: a review. Renew Sust Energ Rev 16(8):5584–5596
8. Jangsawang W, Laohalidanond K, Kerdsuwan S (2015) Optimum equivalence ratio of biomass gasification process based on thermodynamic equilibrium model. Energy Procedia 79:520–527
9. Ruiz JA, Juárez M, Morales M, Muñoz P, Mendívil M (2013) Biomass gasification for electricity generation: review of current technology barriers. Renew Sust Energ Rev 18:174–183
10. Hussain M, Tufa LD, Yusup S, Zabiri H (2018) A kinetic-based simulation model of palm kernel shell steam gasification in a circulating fluidized bed using Aspen Plus®: a case study. Biofuels 9(5):635–646
11. Adeyemi I, Janajreh I (2015) Modeling of the entrained flow gasification: kinetics-based ASPEN Plus model. Renew Energy 82:77–84
12. Doherty W, Reynolds A, Kennedy D (2009) The effect of air preheating in a biomass CFB gasifier using ASPEN Plus simulation. Biomass Bioenergy 33(9):1158–1167
13. Puig-Arnavat M, Bruno JC, Coronas A (2010) Review and analysis of biomass gasification models. Renew Sust Energ Rev 14(9):2841–2851
14. Ramzan N, Ashraf A, Naveed S, Malik A (2011) Simulation of hybrid biomass gasification using Aspen Plus: a comparative performance analysis for food, municipal solid and poultry waste. Biomass Bioenergy 35(9):3962–3969
15. Mohammadidoust A, Omidvar MR (2020) Simulation and modeling of hydrogen production and power from wheat straw biomass at supercritical condition through Aspen Plus and ANN approaches. Biomass Convers Biorefinery:1–17. https://doi.org/10.1007/s13399-020-00933-5
16. Marcantonio V, Monforti Ferrario A, Di Carlo A, Del Zotto L, Monarca D, Bocci E (2020) Biomass steam gasification: a comparison of syngas composition between a 1-D MATLAB Kinetic Model and a 0-D Aspen Plus Quasi-Equilibrium Model. Computation 8(4):86. https://doi.org/10.3390/computation8040086
17. Front Matter A2- Basu P (2010) Biomass gasification and pyrolysis: practical design and theory: Academic Press, USA
18. Baruah D, Baruah D (2014) Modeling of biomass gasification: a review. Renew Sust Energ Rev 39:806–815
19. Paviet F, Chazarenc F, Tazerout M (2009) Thermo chemical equilibrium modelling of a biomass gasifying process using ASPEN PLUS. International Journal of chemical reactor engineering 7(1):40
20. Doherty W, Reynolds A, Kennedy D (2013) Aspen plus simulation of biomass gasification in a steam blown dual fluidised bed. Book Chapter: Materials and processes for energy: communicating current research and technological developments, A. Méndez-Vilas (ed) Formatex Research Centre
21. Begum S, Rasul MG, Akbar D, Ramzan N (2013) Performance analysis of an integrated fixed bed gasifier model for different biomass feedstocks. Energies 6(12):6508–6524
22. Sreejith C, Muraleedharan C, Arun P (2014) Performance prediction of steam gasification of wood using an ASPEN PLUS thermodynamic equilibrium model. Int J Sustain Energy 33(2):416–434
23. Nikoo MB, Mahinpey N (2008) Simulation of biomass gasification in fluidized bed reactor using ASPEN PLUS. Biomass Bioenergy 32(12):1245–1254
24. Im-orb K, Simasatitkul L, Arpornwichanop A (2016) Techno-economic analysis of the biomass gasification and Fischer–Tropsch integrated process with off-gas recirculation. Energy 94:483–496
25. Čeković I, Manić N, Stojiljković D, Trninić M, Todorović D, Jovović A (2019) Modelling of wood chips gasification process in ASPEN Plus with multiple validation approach. Chem Ind Chem Eng Q 25(3):217–228
26. de Andrés JM, Vedrenne M, Brambilla M, Rodríguez E (2019) Modeling and model performance evaluation of sewage sludge gasification in fluidized-bed gasifiers using Aspen Plus. J Air Waste Manage Assoc 69(1):23–33. https://doi.org/10.1080/10962247.2018.1500404
27. Acar MC, Böke YE (2019) Simulation of biomass gasification in a BFBG using chemical equilibrium model and restricted chemical equilibrium method. Biomass Bioenergy 125:131–138
28. Im-orb K, Simasatitkul L, Arpornwichanop A (2016) Analysis of synthesis gas production with a flexible H2/CO ratio from rice straw gasification. Fuel 164:361–373
29. Patra TK, Sheth PN (2015) Biomass gasification models for downdraft gasifier: a state-of-the-art review. Renew Sust Energ Rev 50:583–593
30. Beheshti S, Ghassemi H, Shahsavan-Markadeh R (2015) Process simulation of biomass gasification in a bubbling fluidized bed reactor. Energy Convers Manag 94:345–352

31. Villarini M, Marcantonio V, Colantoni A, Bocci E (2019) ensitivity analysis of different parameters on the performance of a CHP internal combustion engine system fed by a biomass waste gasifier. Energies 12(4):688
32. (2009) Aspen Technology Aspen Plus Dynamic. vol. http://www.aspentech.com/brochures/1716_15_Aspen_Plus_Dynamics_web.pdf, Inc. Accessed April, 2014
33. Rahbari A, Venkataraman MB, Pye J (2018) Energy and exergy analysis of concentrated solar supercritical water gasification of algal biomass. Appl Energy 228:1669–1682
34. Khan Z, Yusup S, Kamble P, Naqvi M, Watson I (2018) Assessment of energy flows and energy efficiencies in integrated catalytic adsorption steam gasification for hydrogen production. Appl Energy 225:346–355
35. Omidvar MR, Meghdadi Isfahani AH (2018) Simulation and modeling of hydrogen production from glucose biomass model compound via hydro-thermal gasification. Energy Equip Syst 6(2):211–219
36. Yucel O, Aydin ES, Sadikoglu H (2019) Comparison of the different artificial neural networks in prediction of biomass gasification products. Int J Energy Res 43(11):5992–6003
37. Elmaz F, Yücel Ö, Mutlu AY (2020) Predictive modeling of biomass gasification with machine learning-based regression methods. Energy 191:116541
38. Elmaz F, Yücel Ö, Mutlu AY (2019) Evaluating the effect of blending ratio on the co-gasification of high ash coal and biomass in a fluidized bed gasifier using machine learning. Mugla J Sci Technol 5(1):1–12
39. Yahaya AZ, Somalu MR, Muchtar A, Sulaiman SA, Daud WRW (2019) Effect of particle size and temperature on gasification performance of coconut and palm kernel shells in downdraft fixed-bed reactor. Energy 175:931–940. https://doi.org/10.1016/j.energy.2019.03.138
40. Shahbaz M, Yusup S, Inayat A, Patrick DO, Ammar M, Pratama A (2017) Cleaner production of hydrogen and syngas from catalytic steam palm kernel shell gasification using CaO sorbent and coal bottom ash as a catalyst. Energy Fuel 31(12):13824–13833
41. Lamminen M, Wood J, Walker H, Chin Y-P, He Y, Traina SJ (2001) Effect of flue gas desulfurization (FGD) by-product on water quality at an underground coal mine. J Environ Qual 30(4): 1371–1381
42. Gao N, Li A, Quan C, Gao F (2008) Hydrogen-rich gas production from biomass steam gasification in an updraft fixed-bed gasifier combined with a porous ceramic reformer. Int J Hydrog Energy 33(20):5430–5438
43. Inayat A, Ahmad MM, Mutalib MA, Yusup S (2012) Process modeling for parametric study on oil palm empty fruit bunch steam gasification for hydrogen production. Fuel Process Technol 93(1): 26–34
44. Weerachanchai P, Horio M, Tangsathitkulchai C (2009) Effects of gasifying conditions and bed materials on fluidized bed steam gasification of wood biomass. Bioresour Technol 100(3):1419–1427
45. McKendry P (2002) Energy production from biomass (part 3): gasification technologies. Bioresour Technol 83(1):55–63
46. Ahmaruzzaman M (2010) A review on the utilization of fly ash. Prog Energy Combust Sci 36(3):327–363
47. Abubakar AU, Baharudin KS (2012) Potential use of Malaysian thermal power plants coal bottom ash in construction. Int J Sustain Constr Eng Technol 3(2):25–37
48. Acharya B, Dutta A, Basu P (2010) An investigation into steam gasification of biomass for hydrogen enriched gas production in presence of CaO. Int J Hydrog Energy 35(4):1582–1589
49. Boerrigter H, Rauch R (2006) Review of applications of gases from biomass gasification. Netherlands
50. Fowler P, Krajačić G, Lončar D, Duić N (2009) Modeling the energy potential of biomass–H2RES. Int J Hydrog Energy 34(16):7027–7040
51. Wilson ED, Clairon Q, Henderson R, Taylor CJ (2018) Dealing with observational data in control. Annu Rev Control 46:94–106
52. Garcia-Perez M, Wang XS, Shen J, Rhodes MJ, Tian F, Lee WJ, Wu H, Li CZ (2008) Fast pyrolysis of oil mallee woody biomass: effect of temperature on the yield and quality of pyrolysis products. Ind Eng Chem Res 47(6):1846–1854
53. Rupesh S, Muraleedharan C, Arun P (2016) gasification of biomass with sorbent enabled CO2 capture. Resourc Efficient Technol 2(2): 94–103
54. Xu G, Murakami T, Suda T, Kusama S, Fujimori T (2005) Distinctive effects of CaO additive on atmospheric gasification of biomass at different temperatures. Ind Eng Chem Res 44(15): 5864–5868
55. Khan Z, Yusup S, Ahmad MM, Chin BLF (2014) Hydrogen production from palm kernel shell via integrated catalytic adsorption (ICA) steam gasification. Energy Convers Manag 87:1224–1230
56. Suwatthikul A, Limprachaya S, Kittisupakorn P, Mujtaba IM (2017) Simulation of steam gasification in a fluidized bed reactor with energy self-sufficient condition. Energies 10(3):314
57. Robinson PJ, Luyben WL (2008) Simple dynamic gasifier model that runs in Aspen Dynamics. Ind Eng Chem Res 47(20):7784–7792
58. Shen L, Gao Y, Xiao J (2008) Simulation of hydrogen production from biomass gasification in interconnected fluidized beds. Biomass Bioenergy 32(2):120–127
59. Inayat A, Ahmad MM, Mutalib MA, Yusup S (2010) Effect of process parameters on hydrogen production and efficiency in biomass gasification using modelling approach. J Appl Sci (Faisalabad) 10(24):3183–3190
60. Moghadam RA, Yusup S, Azlina W, Nehzati S, Tavasoli A (2014) Investigation on syngas production via biomass conversion through the integration of pyrolysis and air–steam gasification processes. Energy Convers Manag 87:670–675
61. Hussain M, Tuf LD, Yusup S, Zabiri H (2019) Characterization of coal bottom ash &its potential to be used as catalyst in biomass gasification. Mater Today Proc 16:1886–1893
62. Lv P, Xiong Z, Chang J, Wu C, Chen Y, Zhu J (2004) An experimental study on biomass air–steam gasification in a fluidized bed. Bioresour Technol 95(1):95–101
63. Shahbaz M, Inayat A, Patrick DO, Ammar M (2017) The influence of catalysts in biomass steam gasification and catalytic potential of coal bottom ash in biomass steam gasification: a review. Renew Sust Energ Rev 73:468–476

Publisher's Note Springer Nature remains neutral with regard to jurisdictional claims in published maps and institutional affiliations.